Study of New Physics Phenomena Decaying in Four-Jet Signatures with the ATLAS Detector

Bachelor Thesis

by

Lisa Vergara

Supervisor:
Dr. Caterina Doglioni

Co-supervisor:
Dr. Charles Kalderon

June 15, 2017

LUND
UNIVERSITY

Division of Particle Physics

Abstract

Particle Physics is well described by the Standard Model (SM). However, there are phenomena in the universe that the model does not describe. Supersymmetry, which predicts a partner particle for all fundamental particles, is an extension of the SM that provides solutions to problems the SM cannot solve. Finding the partner particles is crucial in order to confirm the theory about Supersymmetry. When searching for new low-mass partner particles though, the search is limited by large backgrounds producing similar signatures in the detector, since not all events can be recorded. By recording only necessary jet-information, events become much smaller than entire events, leading to the possibility to save more events. This strategy is called Trigger Level Analysis (TLA).

In this project simulated samples of two top squarks of masses 80 GeV/c^2, decaying into two jets each, were analyzed in order to understand if a Trigger Level Analysis (TLA) could be performed in a four-jet signature. Two different TLA cuts were implemented and compared, where the first one only preserved events with a leading jet with a minimum p_T of 185 GeV/c and three additional jets with a minimum p_T of 85 GeV/c, and the second one preserved events with with a leading jet of a minimum p_T of 185 GeV/c and a subleading jet with a minimum p_T of 85 GeV/c. Analyzing their average mass distributions, a peak at $m_{Avg} = m_{\tilde{t}}$ was found for both, however, the number of events conserved for the TLA cut with the requirements on only the two leading jets was much higher, leading to the conclusion that this option is preferable.

Contents

1 Introduction

Particle physics - the study of the fundamental constituents of matter and the interactions between them - is very well described by the Standard Model (SM) [1]. The Standard Model describes all particles that have been found experimentally so far, and three of the four fundamental forces [1]. Despite all the findings and the correct predictions, the Standard Model is not sufficient enough to describe all the phenomena in our universe, and physics beyond the Standard Model are thus needed [1]. An example of physics beyond the SM, is the proposed Supersymmetry, which predicts that all SM particles have a partner particle. At the Large Hadron Collider (LHC), the most powerful particle accelerator in the world, the search for new physics is ongoing [2, 3]. Here, beams of protons are collided at four intersection points, one of which is at the center of the ATLAS detector [2]. The particle interaction rate in the ATLAS detector is too high for all events to be recorded [4]. Therefore, a trigger system which discards uninteresting events and preserves interesting ones is needed [4]. The problem with this trigger system is that it limits the search for new (undiscovered) low-mass particles, which often produce signatures that resemble background [5]. A new method, which involves analyzing and recording data directly at the trigger level, can help remove this limitation by recording only necessary information [5]. This way, the event size becomes smaller and more events can be recorded [5]. This method is called Trigger Level Analysis (TLA) [5]. The aim of this project was to understand whether it is possible to perform a TLA in a four-jet signature. This was done by analyzing simulated samples of two supersymmetric top quark partners decaying into two quarks each.

In section 2 a theoretical background is presented, with a brief explanation of the Standard Model and examples of physics beyond the Standard Model. Afterwards, experimental aspects are presented: The LHC, the ATLAS detector, the kinematics of particles and this project. The results of this thesis are shown in section 4 and these are followed by conclusions, in section 5.

2 Theoretical Background

2.1 The Standard Model

The Standard Model has been describing particle physics since it was first developed in the early 1970s [1, 6]. It has done so by explaining the properties and interactions of what are today believed to be elementary particles, i.e. particles with no internal structure [1]. These elementary, or fundamental, particles can be divided into three categories: quarks, leptons and gauge bosons [1]. These are shown in figure 1. The first two groups consist of six spin-$\frac{1}{2}$ particles (fermions) each, and their antiparticles, while the particles in the third group are four spin-1 particles (bosons), often called "force carriers" [1, 6]. In addition to these three types of particles, the Standard Model also includes a spin-0 particle: the Higgs boson, which was first observed at CERN in 2012 [1, 6].

The interactions between the fundamental particles are called the fundamental forces of nature [1]. The fundamental forces are four: the strong, weak, electromagnetic and gravitational forces - though only three of these are incorporated in the Standard Model [1, 6]. The force which is not incorporated in the model is the gravitational force; this

force is far weaker than the other three at the energy and length scales probed by particle accelerators today [1, 6]. The remaining forces, the ones that are included in the model, are all associated with the exchange of "force carriers" between the fundamental particles and/or their bound states [1]. The gluons are the massless mediators for the strong interaction, while the photon is the equivalent for the electromagnetic interaction [1]. The mediators for the weak force are two heavy particles called W and Z bosons [1].

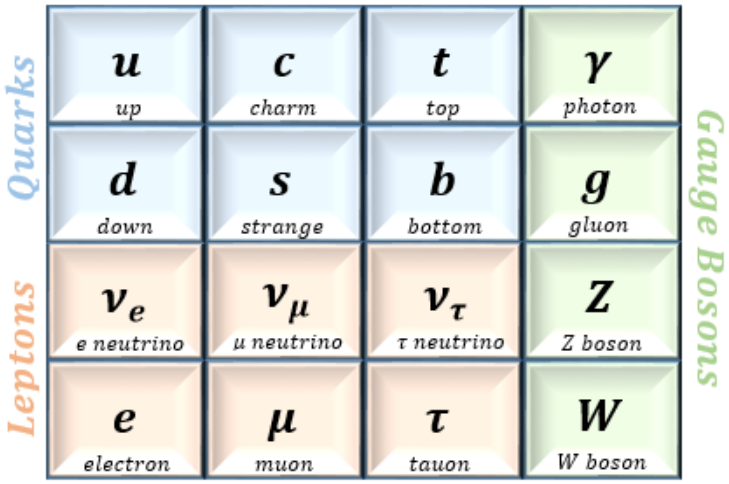

Figure 1: The fundamental particles of the Standard Model.

2.2 Quantum Chromodynamics

Quantum Chromodynamics is the study, within the Standard Model, of the strong interaction - that is, the interaction between quarks and gluons [1, 7]. The gluons, which as mentioned earlier are the mediating particles of this force, couple to an attribute called color charge, which both quarks and gluons possess [1]. Quarks can have three different colors: red, green or blue - or three respective anticolors - while gluons can exist in eight different color states; these states are linear combinations of the mentioned color/anticolor charges [1, 8].

Due to the fact that both quarks and gluons possess color charge, gluons do not only interact with quarks, but also with each other [1]. The consequences of this are two properties named color confinement and asymptotic freedom [1]. Color confinement is the fact that when two colored particles move away from each other, the interaction between them gets stronger [1]. This forbids quarks and gluons - which both have nonzero color charge - from propagating as free particles, and requires bound states to be color neutral or have zero color charge, and to have integer electric charge [1, 7, 8]. The bound states, called hadrons, exist in two types: baryons and mesons [1]. The baryons consist of three quarks, one of each color, and the mesons consist of a quark-antiquark (color-anticolor) pair [1]. Baryons are thus color neutral, while mesons have zero color charge [1]. When the distance between colored particles, also called partons, is short, the interaction between them gets weaker - this is asymptotic freedom [1].

Since the interaction between a pair of quarks increases in strength when pulling them

apart, it becomes easier (energetically) for another quark-antiquark pair to be produced from the vacuum after a certain distance [7, 8]. This new pair then interacts with the original quark pair, creating hadrons in a process called hadronization [7, 8]. In high energy collision experiments, where quarks are generated, this process is repetitive and creates jets of hadrons, which are collimated "showers" of hadrons [7, 8, 9]. These jets reflect the properties of the original particles from which they were created, and they can be observed experimentally [9]. Thus, properties of the original particles can be determined by analyzing jets [9].

2.3 New Physics

The Standard Model is in good agreement with most experimental observations within particle physics today [1]. Still, there are many ways in which the Standard Model could be extended, since there are many phenomena that the model does not describe, for example Dark Matter [1].

One way to extend the model is by trying to unify the strong interaction with the electroweak interaction, which in turn is the unification of the weak and the electromagnetic interactions [1]. The theory of this unification is called the Grand Unified Theory; it requires the coupling constants of the three forces to unify at one point [1, 10]. Although, extremely high energies are needed for this unification to be directly observed, there is already evidence that the strong force becomes weaker at higher energies [11]. The problem is though, that in theory, the coupling constants of the forces do not unify [10].

This problem can be solved by including in the theory a new symmetry of nature called Supersymmetry (SUSY), which in fact, also solves other problems of the Standard Model and provides a Dark Matter particle candidate [1, 10]. Supersymmetry involves doubling the number of fundamental particles by connecting every presently known particle with a supersymmetric partner - or superpartner [1]. This superparticle would differ from its known partner only by half a unit of spin, meaning that the superpartners of fermions are bosons and the superpartners of bosons are fermions, and would otherwise be exactly the same [1]. However, since these new particles have not yet been observed, the masses of the new particles are also expected to be different from the masses of the known partners, due to a symmetry breaking mechanism [1]. The names of the new particles are almost the same as their known partners' names, but a prefix "s" is added to fermions' superpartners and a suffix "ino" is added to the bosons' superpartners [1].

3 Experiment

3.1 The Large Hadron Collider

The largest particle accelerator in the world is the Large Hadron Collider (LHC), located at CERN [2]. It has a circumference of 27 km and collides protons at a center-of-mass energy of 13 TeV, making it the most powerful accelerator in the world [2, 12]. Inside the accelerator, two particle beams traveling in opposite directions are accelerated to extremely high energies and are then made to collide [2]. Strong magnetic fields, which are sustained by superconducting magnets, guide the beams around the accelerator [2].

The magnets are used both to bend the beams around the ring and to focus them [2]. There are four intersection points in the accelerator where the beams are made to collide and four particle detectors are located at these points: ATLAS, CMS, ALICE and LHCb [2].

3.2 Relativistic Mechanics

When particles are accelerated to a velocity which is very close to the speed of light c, as they are in particle accelerators, classical mechanics is no longer valid and has to be extended in order to be compatible with the theory of relativity [13].

Consider two frames of reference: S and S', where the second one is moving in the positive x-direction with constant velocity v, relative to the first. If the two frames coincide at time $t = 0$ and a particle has coordinates (x, y, z, t) in S, the particle will have coordinates (x', y', z', t') in S', where:

$$x' = \gamma(v)(x - vt), \quad y' = y, \quad z' = z, \quad \text{and} \quad t' = \gamma(v)(t - vx/c^2). \tag{1}$$

Here, $\gamma(v)$ is called the Lorentz factor:

$$\gamma(v) \equiv 1/\sqrt{1 - v^2/c^2} \tag{2}$$

The conversion of coordinates between different reference frames is called Lorentz Transformation; its effects are noticeable when the velocity v is comparable to the speed of light and it has "time dilation" and "length contraction" as consequences [1, 14]. In this example, reference frame S' was, for simplicity, chosen to move only in the x-direction. This can be generalized for frames moving arbitrarily [13].

Four-Vectors and Lorentz Invariance

The four-vector for position $\mathbf{X}$, of a particle, is defined as:

$$\mathbf{X} \equiv (x_0, x_1, x_2, x_3) = (x_0, \bar{\mathbf{r}}) = (ct, x, y, z). \tag{3}$$

Since the time t is multiplied with the speed of light, the first component obtains the same unit as the other components of the vector [14]. The velocity four-vector $\mathbf{V}$ is obtained by:

$$\mathbf{V} = \frac{\mathrm{d}\mathbf{X}}{\mathrm{d}\tau} = \frac{\mathrm{d}\mathbf{X}}{\mathrm{d}t} \cdot \frac{\mathrm{d}t}{\mathrm{d}\tau} = \gamma \left(\frac{\mathrm{d}x_0}{\mathrm{d}t}, \frac{\mathrm{d}x_1}{\mathrm{d}t}, \frac{\mathrm{d}x_2}{\mathrm{d}t}, \frac{\mathrm{d}x_3}{\mathrm{d}t} \right) = \gamma(c, \bar{\mathbf{v}}). \tag{4}$$

Where $\mathrm{d}\tau = \mathrm{d}t/\gamma$ and τ is the proper time, i.e. the time according to the particle being observed [14]. A momentum $\bar{\mathbf{p}} = m\bar{\mathbf{v}}$ four-vector $\mathbf{P}$ can also be obtained, by multiplying the velocity four-vector with the rest mass m_0 of a particle:

$$\mathbf{P} = m_0\mathbf{V} = \gamma(m_0 c, m_0\bar{\mathbf{v}}) = \left(\frac{E}{c}, \bar{\mathbf{p}} \right) \tag{5}$$

From this, an energy E term emerges, which is the first component of the four-momentum [14].

As variables change depending on the reference frame from which they are being observed, invariant variables - i.e. variables that are unaffected by Lorentz transformation and are thus the same in all reference frames - are very useful [1]. The proper time, mentioned above is an example of an invariant quantity [14]. The scalar product of four-vectors is also invariant [14]. The scalar product of the four-momentum with itself gives:

$$\mathbf{P} \cdot \mathbf{P} = \left(\frac{m_o c}{\sqrt{1 - v^2/c^2}} \right)^2 - \left(\frac{m_0 \bar{\mathbf{v}}}{\sqrt{1 - v^2/c^2}} \right)^2 = m_0^2 c^2, \tag{6}$$

equation which, in natural units, also can be written as:

$$m_0^2 = E^2 - \bar{\mathbf{p}}^2. \tag{7}$$

This shows that the rest mass m_0 of a particle, also called the invariant mass, is also unaffected by Lorentz transformation [13, 14]. The invariant mass is important for this thesis as it is an observable for this search.

3.3 The ATLAS Detector

One of the intersection points, where beams of protons from the LHC are made to collide, is at the center of the ATLAS detector [15]. The ATLAS detector is a general purpose detector, designed to explore a wide variety of physics, by detecting particles that are created in the mentioned collisions [7, 15]. The detector has a cylindrical form, with a diameter of 25 m and a length of 46 m [15]. It is placed 100 m underground and weighs approximately 7000 tonnes [15].

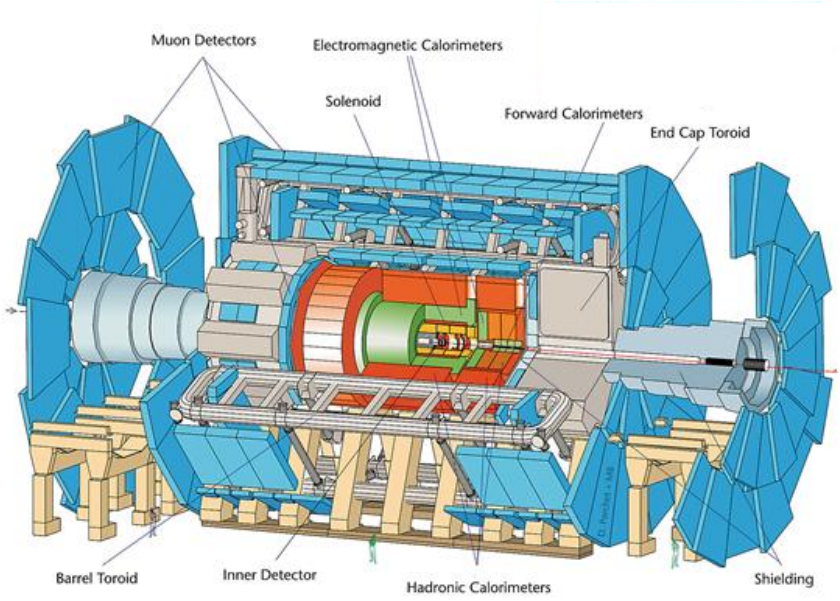

Figure 2: Overview image of ATLAS detector displaying its main components. Figure taken from ref. [16]

The detector consists of several layers of different detecting systems surrounding the collision point [7]. It has four main components: the Inner Detector, the Calorimeter system, the Muon spectrometer and the Magnet System [15]. An overview of the detector is shown in figure 2. The magnet system generates a magnetic field, which bends the particles around the different detecting systems [7]. It consists of a superconducting solenoid and three toroids [7]. The solenoid surrounds the Inner Detector, which measures the momenta, charges and directions of charged particles [7, 15]. The Calorimeter system consists of the electromagnetic and hadronic calorimeters, where the first mentioned is surrounded by the second [7]. Together, the calorimeters measure the energy of electrons, photons and jets [7]. Surrounding the calorimeter system is the Muon spectrometer, which measures the momenta of muons [7].

The ATLAS Trigger System

The proton-proton interaction rate in the ATLAS detector is very high [4]. However, not all events can be recorded due to limited capability of the data recording system [4]. For this reason, a trigger system, which discards uninteresting events and preserves interesting ones, is needed [4].

Originally (during the LHC Run-1) there were three levels in the ATLAS Trigger System: LVL1, LVL2 and the Event Filter (EF) [17]. In the LHC Run-2, the LVL2 and the EF have been merged to the High Level Trigger (HLT) [17]. The first level (LVL1) is a hardware-based trigger that uses information from the calorimeters and the muon detectors [18]. It identifies Regions of Interest: regions where candidate objects (like jets) can be found, and sends the information to the Region of Interest Builder where it can be accessed by the HLT [4, 18]. The High Level Trigger is a software implemented trigger, which can access more detector information than the LVL1 trigger [18]. At the HLT, objects such as jets can be reconstructed [17].

Trigger Level Analysis

As the ATLAS trigger system is developed to record interesting events over a large background of uninteresting ones, the study of new low-mass physics phenomena is limited, due to similar background signatures in the detector [5]. By analyzing and recording information directly at the trigger level, the size of the events can be decreased by including only wanted jet-information [5]. For example, no information from the muon detectors would be included [5]. Since in this case the event size is smaller, more events can be recorded [5]. This method of analysis is called Trigger Level Analysis (TLA) [5].

3.4 Simulated Samples

The simulated event samples for this project were initially created by the ATLAS central production. Events were simulated at the matrix level by MadGraph, which is a Monte Carlo (MC) event generator - so named because it uses MC random number technique to perform integration and sampling from probability distributions, and the name has stuck to refer to all simulations [21]. The stop $\tilde{t}$ (or top squark) is the supersymmetric partner of the top quark t, the heaviest of six quarks [1, 3]. Two stops were simulated, decaying into two quarks each, as shown in figure 3. Thereafter, the parton showers of

each quark were simulated. Parton showers are created when quarks and gluons (partons) are accelerated in proton-proton collisions and emit, for this reason, gluons as radiation [7]. The emitted gluons emit, in turn, more gluons due to confinement [7]. This process, called a parton shower, is repetitive and leads eventually to jets [7]. The simulation of these parton showers was done using Pythia 8, which is another MC event generator [21].

The end result of the initial simulation, was an "EVNT" file, which contained the raw generated event data. This file was then converted, and a "DxAOD" file was produced. The "DxAOD" file was smaller than the "EVNT", as it stored only necessary information, that is, it saved fewer events and only a summary of the information of each event. Lastly, an NTUPLE file was made. This file was written in the ROOT Ntuple format and was even smaller than the "DxAOD", and it was accessible using C++ and Python code and used for the results in this thesis.

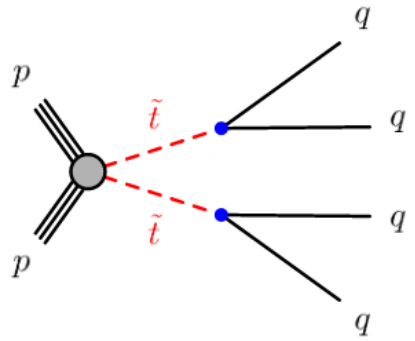

Figure 3: Model of initial simulation created by the ATLAS central production with the Monte Carlo event generator MadGraph. Figure taken from ref. [3]

3.5 Analysis Variables

The ATLAS coordinate system has its origin at the collision point [7]. The beam direction is defined as the z-axis, while the axis pointing from the collision point to the center of the LHC ring is defined as the positive x-axis [7]. The y-axis points upwards from the collision point [7]. The transverse momentum is defined as the momentum in the x-y plane [7]. The polar angle θ is defined to be the angle from the z-axis upwards, but very often the pseudorapity η is used instead of this angle [7]. The pseudorapidity is:

$$\eta = -\ln\left(\tan\left(\frac{\theta}{2}\right)\right). \tag{8}$$

The angle pointing from the x-direction upwards is called the azimuthal angle ϕ [7]. The relationship between the azimuthal angle and the pseudorapidity can be seen as a coordinate system with η on the x-axis and ϕ on the y-axis [22]. Points in this coordinate system represent the direction of outgoing particles; thus a measure of the angular distance between two jets is given by:

$$\Delta R = \sqrt{(\Delta\eta)^2 + (\Delta\phi)^2}. \tag{9}$$

In order to identify two jet pairs ΔR_{min}, defined as :

$$\Delta R_{min} = \sum |\Delta R - 1.0|, \tag{10}$$

should be minimized [3, 22]. Also, the mass asymmetry $\mathcal{A}$:

$$\mathcal{A} = \frac{|m_1 - m_2|}{m_1 + m_2}, \tag{11}$$

where m_1 and m_2 are the invariant masses of the dijets, should be as small as possible for this project [3]. This is because the resonances are expected to have equal masses [3]. The invariant masses can also be used to obtain the average mass of the two reconstructed resonances, as:

$$m_{Avg} = \frac{1}{2}(m_1 + m_2). \tag{12}$$

Another variable that should be defined is the center-of-mass frame production angle $|\cos\theta^*|$ for the stop-pair [3, 23]. Jets that originate from the signal are expected to peak at small values of $|\cos\theta^*|$, while jets originating from the background are expected to have $|\cos\theta^*|$ values close to 1 [3].

3.6 Code Description

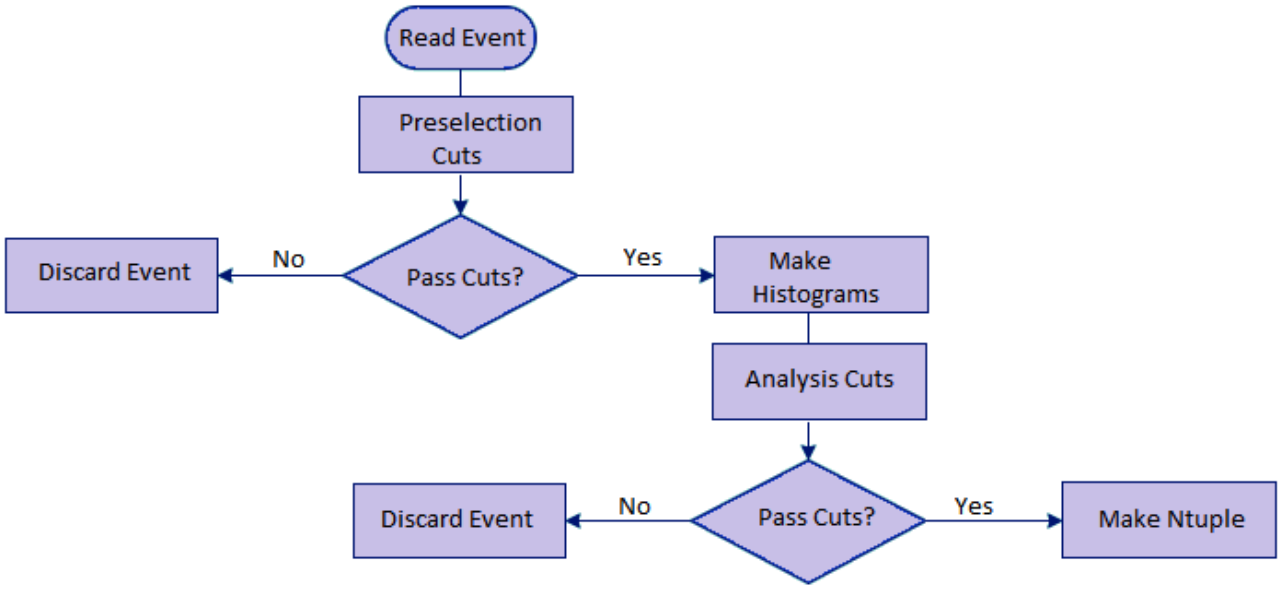

Figure 4: Simplified model of code (Rpv4jResolvedSelector) operation.

In order to analyze the simulated samples, a code "Rpv4jResolvedSelector" that implemented cuts and made histograms was used. Put very simply, the code worked as shown in figure 4. It started by reading one event in the input file and implementing the preselection, or trigger selection, cuts. This meant that only events with at least four jets, with

a certain minimum p_T, were accepted. Events that didn't pass the cuts were discarded, while histograms were made with the ones that did. The analysis cuts were implemented thereafter; this meant that only events with:

- $\eta < 2.4$
- $\Delta R_{min} < 0.003 \cdot m_{Avg}/\text{GeV}$
- $\mathcal{A} < 0.05$
- $|\cos(\theta^*)| < 0.5$

were accepted. At the end, a ROOT Ntuple file was made with the events that passed all the cuts.

3.7 Analysis

In order to understand whether it is possible to perform a Trigger Level Analysis in a four-jet signature, two distributions were analyzed. The first one was the number of events having a given number of jets, to examine whether there were enough events with at least four jets, above a minimum p_T and the second was the average mass m_{Avg} distribution after all analysis cuts.

The code "Rpv4jResolvedSelector" was first ran on the sample files corresponding to a stop mass of 80 Gev/c^2, and then on sample files corresponding to other stop masses, with different p_T cuts. The p_T cuts were:

1. Four jets with a minimum p_T of 120 GeV/c. This choice corresponded to the current trigger selection.

2. Four jets with a minimum p_T of 20 GeV/c. This choice corresponded, in this project, to not applying any cuts on the minimum p_T and thus the number of events passing this cut counted as the "total" number of events in the samples.

3. Leading jet with a minimum p_T of 185 GeV/c, remaining three jets with a minimum p_T of 85 GeV/c. This was the first TLA selection and corresponded to the current TLA selection. [5]

4. Leading jet with a minimum p_T of 185 Gev/c and subleading jet with a minimum p_T of 85 GeV/c. This corresponded to the second option for a TLA selection. [5]

The reason for the 85 GeV/c cuts, in 3 and 4, is so that the multiple interactions within the same LHC collisions do not influence high-p_T jets. More work is needed to use jets with $p_T < 85$ GeV/c in a TLA with real data. After the code had been run, the number of events was plotted as a function of the number of jets and as function of the average mass.

4 Results & Discussion

Figures 5 and 6 show four histograms each, made from the samples where the simulated stop has a mass of 80 GeV/c^2. The different histograms represent the number of events present after different p_T cuts are applied.

In figure 5, the histograms are made already after the preselection/trigger cut (as shown in figure 4) and they depict the number of events present with a certain number of jets. As can be seen, the number of events differs significantly between the first p_T cut and the the second p_T cut, clearly showing why the current trigger system does not favor the search for new low-mass resonances. When looking at the first TLA selection, p_T cut 3, it can be seen that even if more events are saved than with the current trigger, the first TLA option still removes many events. Thus, the first TLA selection is not an optimal option when searching for new low-mass resonances either. The second TLA option, on the other hand, saves many more events, but will need more work to be used in ATLAS.

Figure 6 shows the existing number of events with a certain average mass. Unlike the histograms in figure 5, the histograms in figure 6 are made after both the trigger and the analysis cuts have been applied. For real detector data, a peak at $m_{Avg} = m_{\tilde{t}}$ would be expected for a signal, therefore the height of the peaks (or the number of events at the stop mass) shows that performing a TLA on a four-jet signature is possible. If the peaks are high enough, the possibility of distinguishing them from the background is greater. The peaks in the histogram corresponding to the first and third cut are low, thus distinguishing these in real detector data would probably not be possible due to large background. The peaks in the histograms corresponding to the second and fourth cut on the other hand, are high enough and would most probably be observable in real detector-data.

In figures 7b-f and 8b-f the same histograms are shown as in figure 5 and 6, respectively, although here, the mass of the simulated stop is: (b) 175 GeV/c^2, (c) 200 GeV/c^2, (d) 500 GeV/c^2, (e) 650 GeV/c^2 and (f) 1000 GeV/c^2. Figures 7a and 8a show the p_T cuts (same as above).

In figure 7 it can be observed that, as the mass of the stop increases, the difference between the number of events, for the different p_T cuts, decreases. For masses 175 and 200 GeV/c^2 a second option TLA (applying the fourth p_T cut) may still be advantageous, but for the higher masses ($\geq$ 500 GeV/c^2) the number of events preserved is essentially the same for all cuts, specially in the case for $m_{\tilde{t}} = 1000$ GeV/c^2, therefore a TLA is not needed.

When it comes to the histograms in figure 8, the same observation as in figure 7 can be made; as the mass of the stop increases, the difference between the number of events for the different p_T cuts decreases and in this case this eventually leads to the same average mass distributions for all the cuts. For masses 175 and 200 GeV/c^2, the distributions still differ and the peaks of the second and fourth cuts are still the highest peaks. For the higher stop masses ($\geq$ 500 GeV/c^2) the distributions start looking the same for the different cuts, meaning that even in a four-jet signature all events are preserved with the current trigger system.

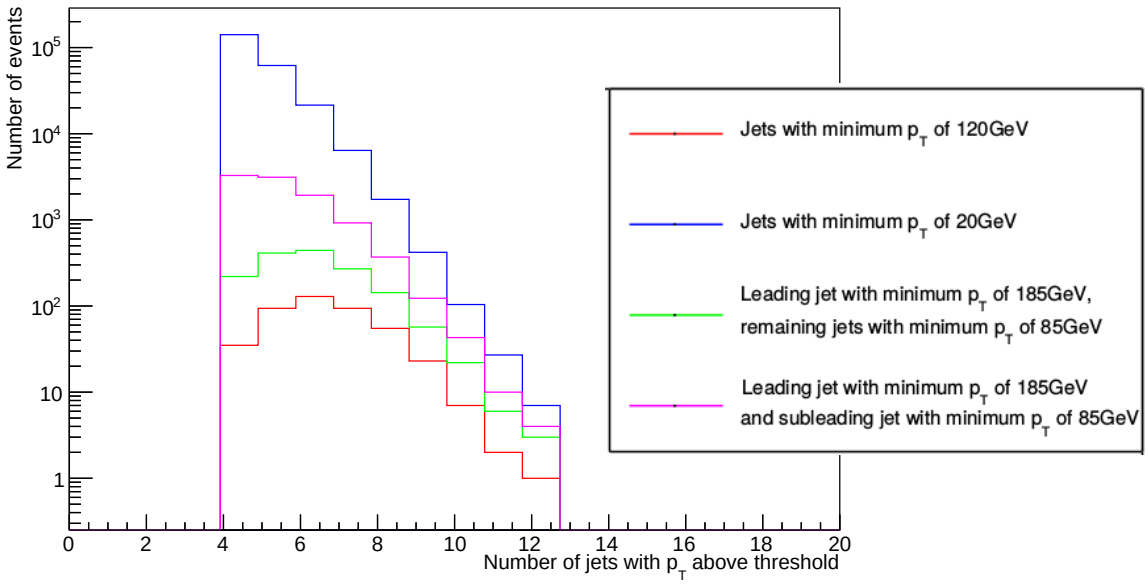

Figure 5: Histograms made after different p_T preselection cuts, depicting number of events with certain number of jets, for samples with $m_{\tilde{t}}$=80 GeV/c^2

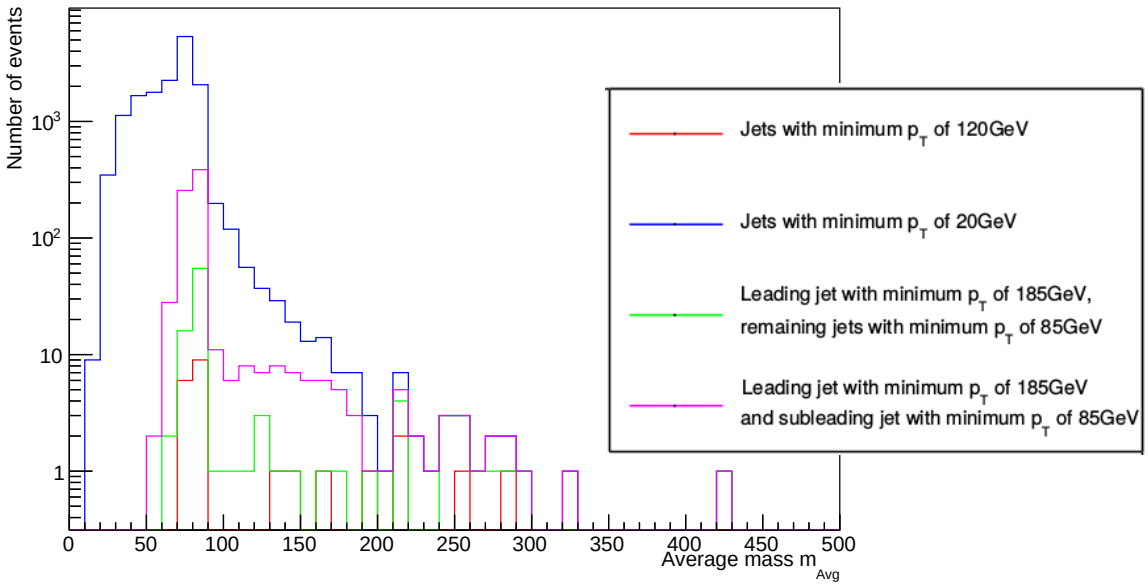

Figure 6: Histograms made after different p_T preselection cuts and after analysis cuts, depicting number of events with certain average mass, for samples with $m_{\tilde{t}}$=80 GeV/c^2

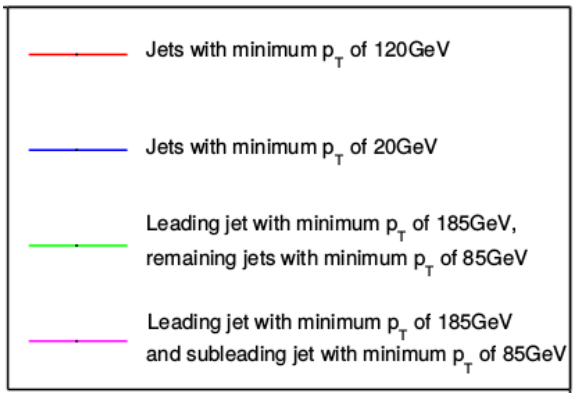

(a) p_T cuts

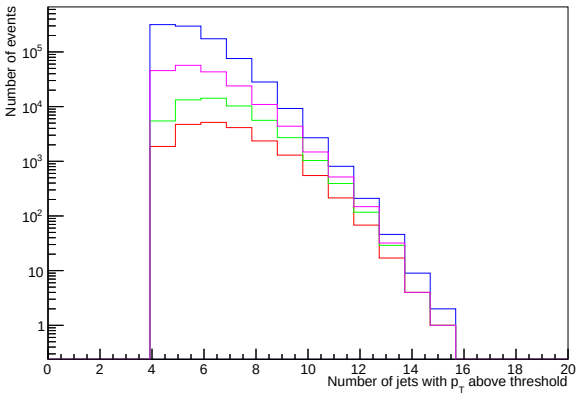

(b) $m_{\tilde{t}}$=175 GeV/c^2

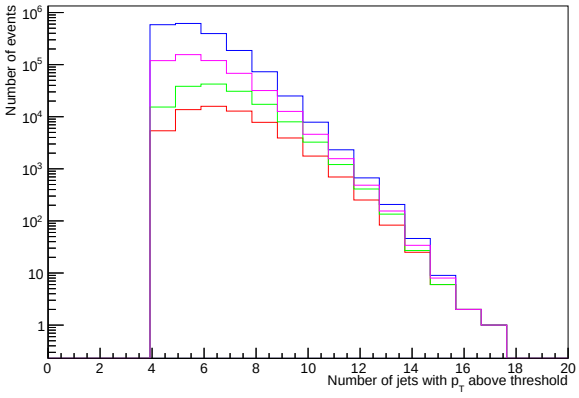

(c) $m_{\tilde{t}}$=200 GeV/c^2

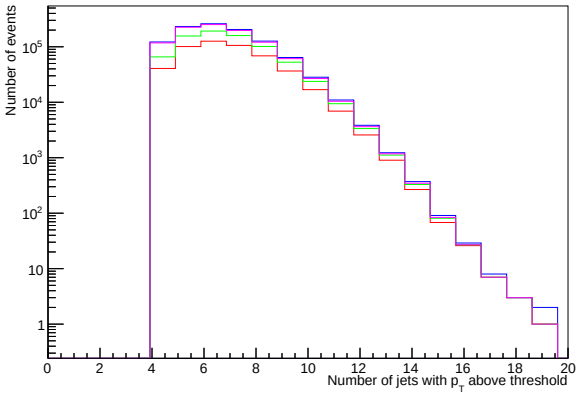

(d) $m_{\tilde{t}}$=500 GeV/c^2

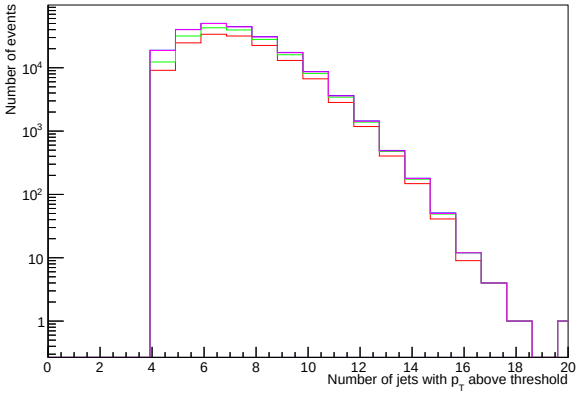

(e) $m_{\tilde{t}}$=650 GeV/c^2

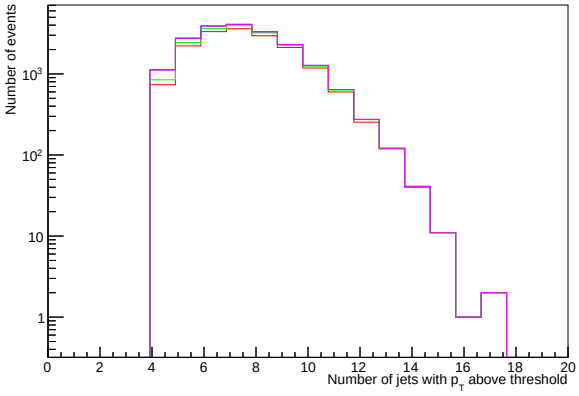

(f) $m_{\tilde{t}}$=1000 GeV/c^2

Figure 7: Histograms made after different p_T preselection cuts, depicting number of events with certain number of jets, for samples with different stop masses.

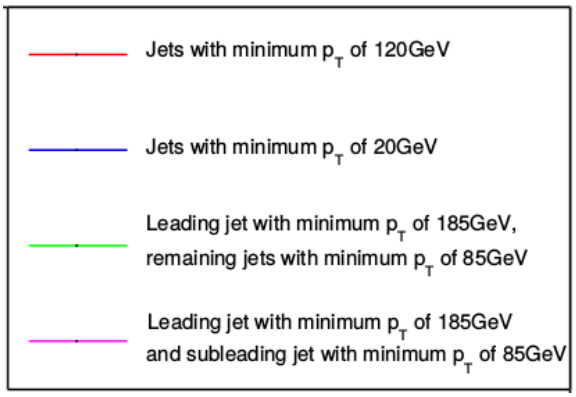

(a) p_T cuts

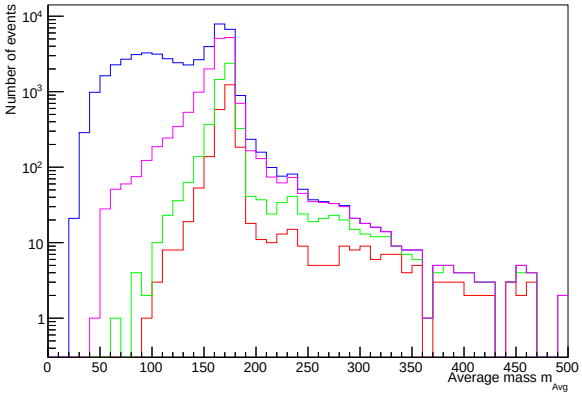

(b) $m_{\tilde{t}}$=175 GeV/c^2

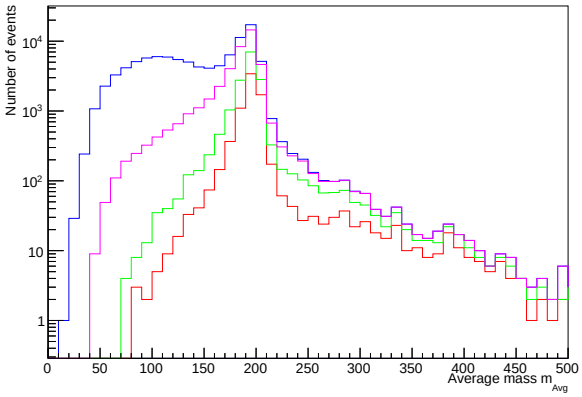

(c) $m_{\tilde{t}}$=200 GeV/c^2

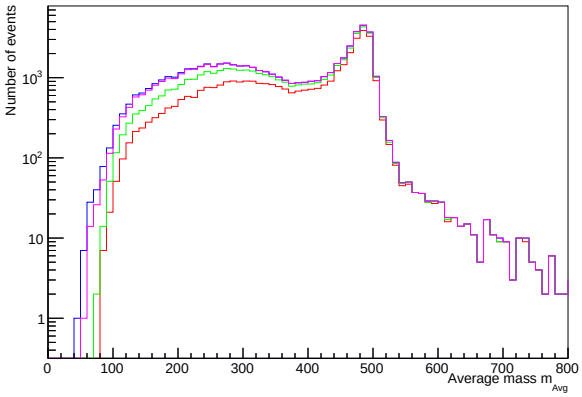

(d) $m_{\tilde{t}}$=500 GeV/c^2

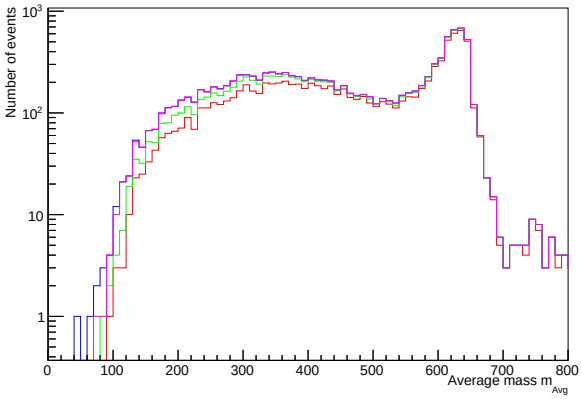

(e) $m_{\tilde{t}}$=650 GeV/c^2

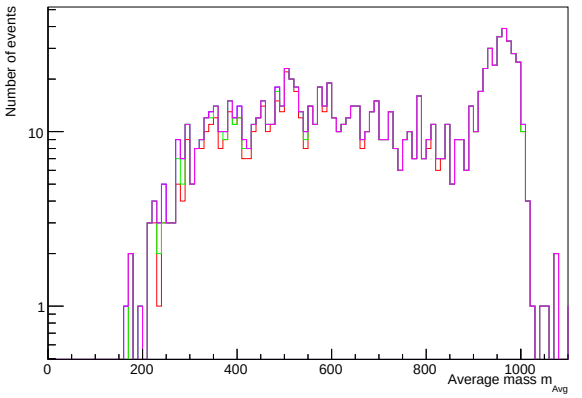

(f) $m_{\tilde{t}}$=1000 GeV/c^2

Figure 8: Histograms made after different p_T preselection cuts and after analysis cuts, depicting number of events with certain average mass, for samples with different stop masses.

5 Summary & Conclusion

When searching for new low-mass physics phenomena with the ATLAS detector, the search is limited by the trigger system, since the low-mass resonances produce signals which are similar to background and are, for that reason, discarded. The aim of this project was to understand whether this limitation could be removed in a four-jet signature by performing a Trigger Level Analysis.

This was analyzed by implementing two different TLA cuts on simulated samples of two top squarks $m_{\tilde{t}}$ of masses 80 Gev/c^2. The squarks would decay into two jets each and when implementing the first TLA cut, only events with a leading jet with a minimum p_T of 185 GeV/c and three more jets with a minimum p_T of 85 GeV/c would be preserved. When implementing the second TLA cut, events with a leading jet with a minimum p_T of 185 GeV/c and a subleading jet with a minimum p_T of 85 GeV/c would be preserved. The average mass distributions of these two cuts were compared to each other and a peak was found at $m_{Avg} = m_{\tilde{t}}$ in the histograms corresponding to both cuts. When looking at the number of events preserved though, it could be observed that when implementing requirements only on the two leading jets, the number of events conserved was much higher than it was otherwise. Therefore a conclusion could be drawn that performing a TLA on a four-jet signature should be possible when implementing the right cuts, and in this case the best option (of the ones analyzed) would be preserving all events with a leading jet and a subleading jet with minimum p_T of 185 and 85 GeV/c, respectively.

Only demanding the two leading jets to have a minimum p_T can also mean that the decay products of each top squark merged. This poses a new challenge, since the current selection may not be optimal to distinguish signal from background, as it has been optimized for final states with four well separated jets. For future work, understanding how to investigate these jets substructures could be of importance in order to find the searched resonances.

References

[1] Martin B.R, Shaw G. Particle Physics. Third edition. Chichester, United Kingdom: John Wiley & Sons Ltd; 2008

[2] CERN. The Large Hadron Collider [Internet]. 2014 [cited 2016 Dec 3]. Available from: http://cds.cern.ch/record/1998498

[3] ATLAS Collaboration. A search for pair produced resonances in four-jet final states in proton-proton collisions at $\sqrt{s} = 13$ TeV with the ATLAS experiment [Internet]. 2016 [cited 2016 Dec 7]. Available from: https://cds.cern.ch/record/2206277

[4] Armstrong S, Assamagan K, Baines J.T, Bee C.P, Biglietti M, Bogaerts A, et al. Architecture of the ATLAS High Level Trigger Event Selection Software. Nucl Instrum Meth A [Internet]. 2004 [cited 2016 Dec 7]; 518(1-2): 537-541. DOI: 10.1016/j.nima.2003.11.079. Available from: http://www.sciencedirect.com/science/article/pii/S0168900203029462

[5] ATLAS Collaboration. Search for light dijet resonances with the ATLAS detector using a Trigger-object Level Analysis in LHC *pp* collisions at $\sqrt{s} = 13$ TeV [Internet]. 2016 [cited 2016 Dec 8]. Available from: http://inspirehep.net/record/1470774/

[6] CERN. The Standard Model [Internet]. 2012 [cited 2016 Nov 16]. Available from: http://cds.cern.ch/record/1997201

[7] Boelaert N. Dijet angular distributions in proton-proton collissions at $\sqrt{s} = 7$ TeV and $\sqrt{s} = 14$ TeV. Lund University; 2010.

[8] Henrichs A.C. Top Quark Pair Production. Switzerland: Springer International Publishing; 2014

[9] Ali A, Kramer G. Jets and QCD: A historical review of the discovery of the quark and gluon jets and its impact on QCD [Internet]. Eur Phys J H; 2011 [cited 2016 Nov 30]. Available from: https://arxiv.org/abs/1012.2288v2

[10] de Boer W. Grand Unified Theories and Supersymmetry in Particle Physics and Cosmology [Internet]. 1994 [cited 2016 Dec 1]. Available from: https://arxiv.org/abs/hep-ph/9402266v5

[11] CERN. Unified forces [Internet]. 2012 [cited 2016 Dec 1]. Available from: http://cds.cern.ch/record/1997194

[12] ATLAS Collaboration. Search for new phenomena in dijet mass and angular distributions from pp collisions at $\sqrt{s} = 13$ TeV with the ATLAS detector [Internet]. 2016 [cited 2016 Dec 3]. Available from: https://arxiv.org/abs/1512.01530

[13] Jönsson L. Lectures in Particle physics [Internet]. [updated 2016; cited 2016 Dec 6]. Available from: http://www.hep.lu.se/staff/christiansen/teaching/leif_fysc14_autumn_2016.pdf

[14] Shankar. Relativity Notes [Internet]. 2006 [cited 2016 Dec 6]. Available from: http://oyc.yale.edu/sites/default/files/notes_relativity_4.pdf

[15] ATLAS. Detector and Technology [Internet]. [cited 2016 Dec 4]. Available from: http://atlas.cern/discover/detector

[16] CERN. Layout of ATLAS [Internet]. 1997 [updated 2013 Dec 13; cited 2016 Dec 5]. [Figure]. Available from: https://cds.cern.ch/record/39038

[17] Nakahama Y. The ATLAS Trigger System: Ready for Run-2. J. Phys [Internet]. 2015 [cited 2016 Dec 18]. DOI: 10.1088/1742-6596/664/8/082037. Available from: http://iopscience.iop.org/article/10.1088/1742-6596/664/8/082037/pdf

[18] Hauser R. The ATLAS trigger system. Eur Phys J C [Internet]. 2004 [cited 2016 Dec 7]; 34(1): 173-183. DOI:10.1140/epjcd/s2004-04-018-6. Available from: http://link.springer.com/article/10.1140/epjcd/s2004-04-018-6

[19] Kersevan B.P. Using the ATLAS Computing Model. 2015 [cited 2016 Dec 9]. Available from: https://indico.cern.ch/event/352570/contributions/828874/attachments/698267/958816

[20] GoldSim Technology Group. What is the Monte Carlo method? [Internet]. 2016 [cited 2016 Dec 9]. Available from: http://www.goldsim.com/Web/Introduction/Probabilistic/MonteCarlo/

[21] Seymour M.H, Marx M. Monte Carlo Event Generators [Internet]. 2013 [cited 2016 Dec 9]. Available from: https://arxiv.org/abs/1304.6677

[22] Jones D, Vallejo R. Study of Transversal Momentum, Phi and Eta: An In-Depth Look Into How To Identify and Calculate [Internet]. 2014 [cited Dec 10]. Available from: https://www.i2u2.org/elab/cms/posters/display.jsp?type=paper&name=study_of_transversal_mom cms-daisy-fetsko-mills_godwin_high_school-henrico-va-2014.0302.data

[23] ATLAS Collaboration. A search for top squark with R-parity-violating decays to all-hadronic final states with the ATLAS detector in $\sqrt{s} = 8$ TeV proton-proton collisions. JHEP [Internet]. 2016 [cited Dec 10]. DOI: 10.1007/JHEP06(2016)067 Available from: https://arxiv.org/abs/1601.07453